Analytical Methods

Accepted Manuscript

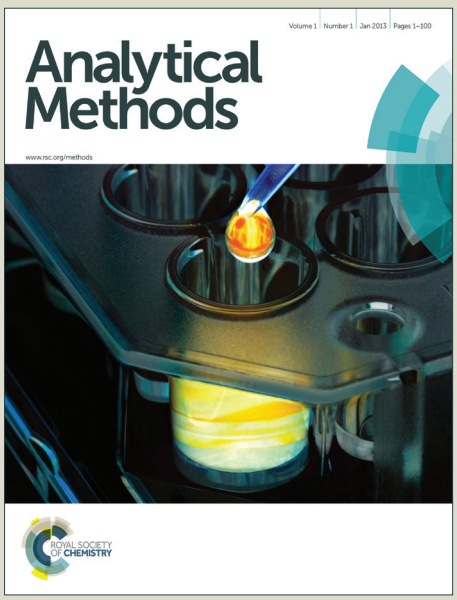

ROYAL SOCIETY OF CHEMISTRY

www.rsc.org/methods

Determination and analytical validation of creatinine content in serum using image analysis by multivariate transfer calibration procedures

Camilo de Lelis Medeiros de Morais and Kássio Michell Gomes de Lima*

Universidade Federal do Rio Grande do Norte, Instituto de Química, Grupo de Pesquisa em Química Biológica e Quimiometria, CEP 59072-970 Natal, RN, Brazil

Abstract: The main objective of this study was to explore the feasibility of image analysis (RGB, HSI and gray intensity histograms) and partial least squares regression using a calibration model transfer technique in quantitative analysis of creatinine in serum samples by the use of two different devices: a desktop scanner and a cell phone camera. In addition, a multivariate validation based on linearity, accuracy, sensitivity, bias, prediction uncertainty and β-expectation tolerance intervals were estimated. The colorimetric reaction for creatinine was carried out in a 96-microwell plate format with flat-bottomed 250 μL microwells. The results achieved separately for both devices were very significant compared to the reference method, showing no statistical difference at a confidence level of 95%. When the calibration model based on the scanner was used directly to predict the concentration for cell phone data, it produced an unsatisfactory prediction with the RMSEP = 0.79 mg dL^{-1}. However, the prediction were greatly improved after the calibration was transferred based on DS (RMSEP = 0.14 mg dL^{-1}). The same trend was observed when the scanned data were predicted by the calibration model based on the cell phone, where the initial RMSEP = 0.25 mg dL^{-1} was reduced to RMSEP = 0.10 mg dL^{-1}, after calibration transfer. These results shows the transferability of the calibration transfer technology applied to image data, where efficient calibration transfer to other devices was clearly demonstrated with all devices in the study effectively giving similar results on a transfer set.

Key-Words: creatinine; calibration transfer; direct standardization; cell phone; scanner; validation;

* Corresponding author. Tel.: +55 84 3342 2323;

E-mail address: kassiolima@gmail.com (K.M.G Lima)

2

Graphical Abstract

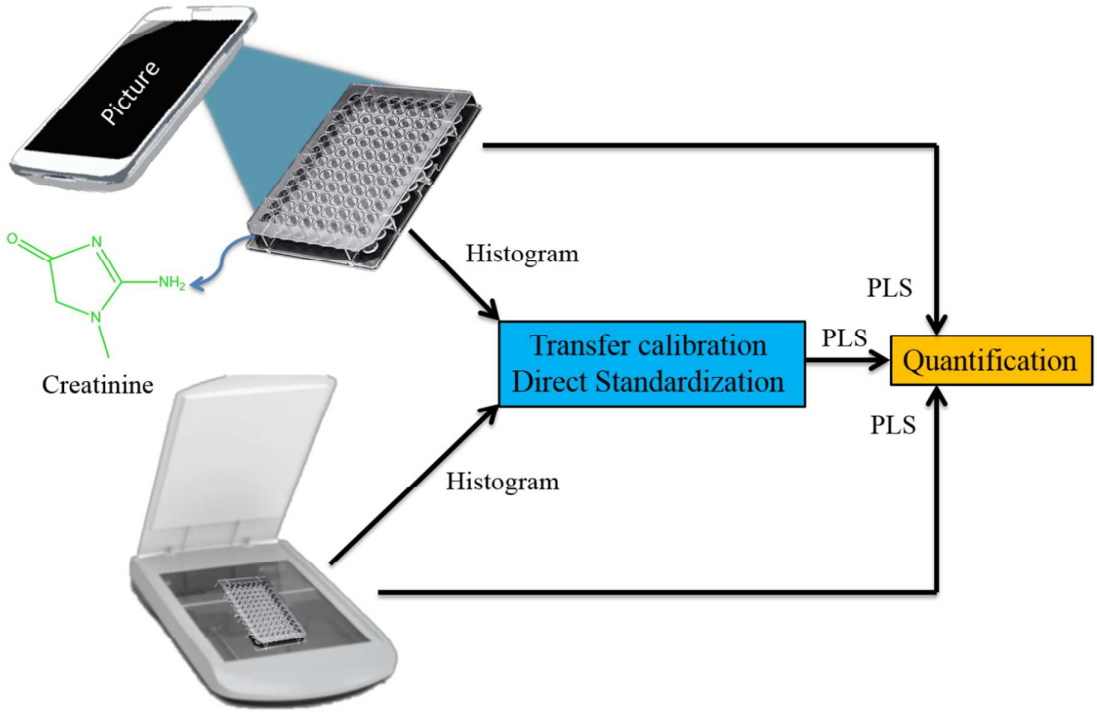

1. Introduction

Creatine (α-methyl-guanidinoacetic acid) is synthesized in the liver, pancreas, and kidneys from the amino acids arginine, glycine, and methionine. Creatinine is produced as a waste product of creatine and phosphocreatine. Because much of the creatinine is produced in muscle, the amount of creatinine that is measured in blood is proportional to the patient's lean muscle mass. The waste product, creatinine, enters the blood supply, where it is removed through the kidneys. It is regarded as the most useful way to deduce the efficiency of the kidneys and to diagnose renal failure.[1]

Several works have been reported in literature exploring the use of high-performance liquid chromatography,[2] nuclear magnetic resonance,[3] Fourier transform infrared,[4] near infrared spectroscopy[5], Raman spectroscopy,[6] and square wave voltammetry,[7] among others[8,9], for quantifying creatinine within blood and urine. However, most of these techniques are highly-sophisticated, expensive, immobile, or require rigorous pre-treatment sampling, all of which are potential hurdles to overcome in providing a cheap, simple and portable detection method for creatinine in point-of-care diagnostics.

Another possibility for measuring plasma creatinine is through endpoint colorimetrics by direct color formation with picric acid, known as the Jaffe reaction.[10] In the Jaffe reaction, creatinine reacts with picric acid in an alkaline environment to generate an orange-red product, as shown in Figure 1. Color intensity of the orange-red product is proportional to original concentration of creatinine in solution, a standard curve which can be created and used to calculate the creatinine content of an unknown sample. Advantages of this method are its cost effectiveness and ease of performance.

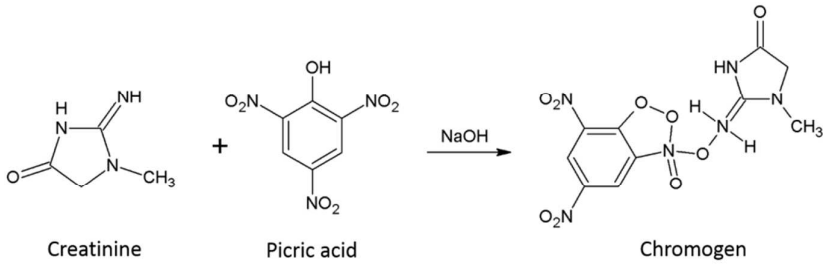

Figure 1: Jaffe reaction for determination of creatinine.

Nowadays, digital imaging is becoming more important because of its ability to carry out fast and non-invasive low-cost analyses on biochemical assays. The fast growth of communication technologies all over the world have especially increased the number of papers published exploring the uses of webcams,[11] scanners[12], cell phones[13] and digital cameras to investigate the optical properties of colorimetric assays and other applications[14–16]. These digital images are translated into millions of colors using basically three standard models: RGB (R—red, G—green and B—blue),[17] the HSI (H—hue, S—saturation and I — intensity)[18] and the grayscale.[19]

One interesting approach for digital analysis is related to the use of color histograms.[20,21] It describes the statistical distribution of the pixels as a function of the recorded color component, and not the direct physical–chemical behavior. The application of color histograms for colorimetric test has great potential for many applications which involve producing chemical color changes. Other approaches, several standard colorimetric reactions for biochemical assays using a webcam, scanner, cell phones and digital camera have been miniaturized to be used with microwells on microplates.[12] The advantages of this approach can be described as a reduction in the amount of reagents and waste due to the low amount of total reagent (250 μL), reduction in costs (microplate price for a base unit - US$ 4.00) and an increase in the analytical frequency because image analysis with a microplate has the potential to perform 96 tests at the same time.

However, in almost any digital imaging procedure designed to make a quantitative measurement, the first step involves performing a calibration. A practical limitation in calibration occurs when an existing model is applied to spectra that were measured under new environmental conditions or on a separate instrument.[22] The responses, for instance, from two instruments for the same sample measured under the same conditions will be different and multivariate calibration models will therefore not necessarily be valid for this new situation. An alternative is to apply chemometric techniques to correct for instrumental and environmental differences, thereby making the model transferable and avoiding full recalibration.[23] In the case of digital image transfer, the response of a sample measured on the slave scanner-device is corrected to the response obtained on the master scanner-device so that the image of standards collected on the master and slave instruments resemble each other. Different multivariate standardization approaches such as direct standardization (DS)[24] and piecewise direct standardization (PDS)[25] have been used to solve the problem of transferability when there are quite different instruments involved. Basically, these standardization methods transform the spectra or image of a new instrument to resemble those from the original instrument.

Therefore, the objectives of this paper were three-fold: (1) to implement the multivariate calibration transfer using color histograms (RGB, HSI and gray intensity histograms) between two optical devices (camera cell phone and desktop scanner)based on a DS procedure for the determination of creatinine in serum samples adapted to a 96-microwell plate; (2) to compare the errors of prediction and bias of an independent test set of creatinine acquired from both the master (desktop scanner) and slave (cell phone) devices after applying the conventional DS correction; (3) to validate a multivariate image analysis (MIA) method based on digital images estimating the linearity,

accuracy, sensitivity, bias, prediction uncertainty and b-expectation tolerance intervals. To the best of our knowledge, this is the first demonstration of determination and analytical validation of creatinine content in serum using color histograms measured by cell phone and scanner by multivariate transfer calibration procedures.

2. Material and Methods

Samples

The colorimetric reaction for determination of creatinine was performed using a commercial kit that contains an immobilized biochemical compound and color reactants. The kit was acquired from Labtest® (Labtest Diagnóstica SA, Brazil)[26] with reference code ref. 35. The standard of creatinine contained in this kit is traceable to Standard Reference Material (SRM) 914 from the National Institute of Standards and Technology (NIST).The reference tests were performed using the standard method of the company according to the modified Jaffe method[10], where a yellowish red complex is formed after creatinine reacts with picric acid whose absorption at 510 nm is proportional to the concentration. The reference calibration procedure was done according to recommendations of the National Kidney Disease Education Program (NKDEP) for standard dosage of creatinine in serum.[27] The range of concentration studied was from 0.03 to 4.00 mg dL^{-1},being fourteen samples for calibration set and six for validation set acquired in triplicate, which covers the level of desirable creatinine in serum for adults (0.70 – 1.20 for males, 0.53 – 1.00 for females), according to Labtest's diagnostic kit. Creatinine concentration out of these levels can be an indicator of renal disease.

For colorimetric tests, microcentrifuge tubes were filled with (i) 0.25 mL of creatinine sample; (ii) 2.0 mL of buffer solution (sodium hydroxide 20.8 mmol L^{-1} and sodium tetraborate 12.7 mmol L^{-1}); and (iii) 0.5 mL of picric acid 44.4 mmol L^{-1}. Next, the tubes were vortexed and incubated for 10 min at 37ºC. Then, 250 µL of solution was inserted into the microwells of a 96-well ELISA microplate (Fisher Scientific, USA) for imaging analysis. For reference measurements, a UV-Vis spectrophotometer Evolution 60S (Thermo Scientific, USA) was used with a bucket filled with all of the micro centrifuged content (2.75 mL).

Digital image acquisition

The images of ELISA microplate were acquired by scanner and a cell phone device. For the scanner, the microplate was scanned by a conventional HP Scanjet G2410 desktop scanner (Hewlett-Packard, USA) in which the images were saved in .TIFF format at 72 x 72 dpi. The scanned images were then loaded into MATLAB® software version 7.12 (MathWorks, USA) and the regions of interest (ROIs) composed of a squared region of 21 x 21 pixels of each microwell were automatically cropped by a homemade algorithm. For the cell phone, ELISA microplate images were acquired by a Smartphone Samsung Galaxy Y 2.0 Megapixel camera. The photos were acquired from a distance of about 15 cm from the camera to the top of the microplate above a white surface by using 2x zoom, with the device held in a static position to avoid blur. The images in .JPEG format at 96 x 96 dpi were then transferred to a computer where the ROIs were cropped with the size of 10 x 10 pixels using GIMP 2.0 software.[28] Thereafter, the ROIs were loaded into MATLAB and the chemometric models were built. In addition, background images of the ELISA microplate with a size of 21 x 21 and 10 x 10 pixels were also acquired from both devices, respectively. These images did not have any reactant content, only the microplate surface.

In order to avoid external light interfering on the microplate surface, the image acquisition process by desktop scanner was carried out with the scanner lid closed. For cell phone data, ambient light has an effect under the image, however this interference was corrected by histogram normalization and the application of multivariate calibration instead of regular univariate model.

Data analysis

After the images from both devices were loaded into MATLAB, the color histograms for Gray-Red-Green-Blue-Hue-Saturation-Intensity channels of each image at a concentration level were acquired. Twenty images of creatinine were obtained within the studied concentration range for each device, where fourteen of these were used in calibration set and six in prediction set, according to the Kennard-Stone algorithm.[29]

The histograms of each image were concatenated into a unique array according to the order previously mentioned. The sample histograms were normalized subtracting the histogram of the background images from it. This was done to reduce the effect of shadows on the microplate surface which can mask the real color information of the samples. Next, the normalized histograms were arranged into an $\mathbf{X}$ $\{m \times n\}$ matrix containing m histograms at a different concentration level, with length of n variables. The calibration model for each device was made using partial least squares (PLS) regression with 3 latent variables and mean center preprocessing applied to $\mathbf{X}$ matrix. These models were built using PLS Toolbox 7.0.3 (Eigenvector Research, Inc. USA) in MATLAB.

Standardization

Several steps in the standardization and multivariate calibration transfer for creatinine estimation between camera cell phone and desktop scanner devices were carried out. Initially, a small number of calibration samples were selected and used in the transfer set. A standardization matrix was calculated from the digital image of subset samples measured on both devices. Direct standardization (DS) algorithm[30] was used, in which each histogram was constructed from several histograms in a small window of the digital image measured on each device. The standardization matrix was used to correct the digital image measured on both devices to account for instrumental and measurement differences. As a result of the standardization, a new set of histograms ('standardized' histograms) were obtained as if they were measured on either of these devices. The technique chosen for selection of transfer samples considered in this study was the classic Kennard Stone (KS) algorithm. The cell phone was treated as the master (M) device, and the scanner as the slave (L) device. The calibration model was transferred from the cell phone to the scanner. The following abbreviations will also be employed:

RMSEP Root mean square error of prediction

$RMSEP^{S}_{M}$ RMSEP for the prediction set of device cell phone, employing the model calibrated for device scanner. Cell phone and scanner can be either master (M) or slave (L)

$RMSEP^{S}_{MT}$ RMSEP for the prediction set of device cell phone, employing the model calibrated for device scanner with the use of transfer samples.

Multivariate analytical validation

The following figures of merit have been calculated to evaluate and validate the method: root means squared error of cross validation (RMSECV) or in the external

validation (RMSEP), based on linearity, accuracy, sensitivity, bias and prediction uncertainty. For brevity in this study, the β-expectation tolerance intervals[31] were included, and was calculated as follows:

$$\beta - TI = RE(\%)_j \pm t\sqrt{1+\frac{1}{pnB_j^2}RSD(\%)_j} \quad (1)$$

where p is the number of series, n is the number of independent replicates per series, RE (%) is the mean relative error for the n replicates for the j_{th} level, RSD (%) is the relative standard deviation for the n replicates for the j_{th} level. t is bicaudal t-student critical values for m degrees of freedom. ν is calculated according to the equation below:

$$\nu = \frac{(R_J+1)^2}{\frac{\left(R_j+\frac{1}{n}\right)^2}{p-1}+\frac{\left(1-\frac{1}{n}\right)}{pn}} \quad (2)$$

where R_J is the ratio between within series variance and between series variance, and B_J is estimated using R_J

$$B_J = \sqrt{\frac{R_J+1}{nR_J+1}} \quad (3)$$

Based on β-TI, the accuracy profile makes a visual and reliable representation of the actual and future performances of the analytical method possible, and thus enables better risk management. The use of β-TI as an innovative figure of merit has recently been extended to multivariate calibration, mainly focused on the validation of NIR methods in pharmaceutical analysis[32] and application of digital images in food analysis.[33]

3. Results and Discussion

3.1 Univariate model

A univariate calibration for both devices (cell phone and scanner) was previously attempted for the construction of the multivariate model for the feasibility of image analysis (RGB, HSI and gray intensity histograms) using a calibration model transfer technique in quantitative analysis of creatinine in serum samples. In the univariate calibration, the normalized histograms correspondent to the intensity of channels (RGB, HSI and gray intensity) were chosen and plotted against its measured concentration value. For building the univariate model, the sample histograms were divided into 14 for the calibration set and 6 for the validation set by using the Kennard–Stone algorithm, which assured the presence of the most representative samples in the calibration set through a uniform scanning of the independent variables data set. A linear fit was then made defining a linear equation which represented the regression. We extracted the intensity of prediction samples and found their concentrations by a linear equation of calibration. Then, we conducted a statistics relation with the real concentration measured by the reference method (enzymatic colorimetric). Poor correlations and high relative errors were found for the univariate models, and were not considered satisfactory for quantification. So, we built the PLS model and an observed an improvement for the multivariate model.

3.2 Multivariate model

For building the PLS model, no preprocessing other than mean centering was applied to the histograms. Figure 2 shows the typical histogram for each device.

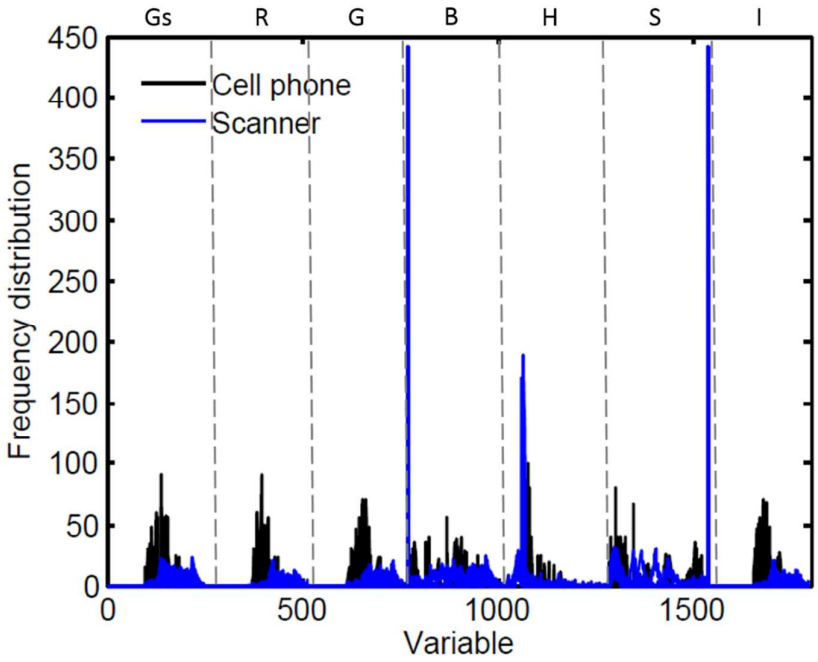

Figure 2: Frequency distribution per length of the color histograms for grayscale (Gs), Red (R), Green (G), Blue (B), Hue (H), Saturation (S), and Intensity (I) channels used in chemometric treatment for: (−) Cell phone; and (−) Scanner.

The histogram profiles shown in Figure 2 for cell phone and scanned images are very different, where the signal for scanner data are more intense in Blue, Hue, and Saturation channels. For cell phone data, the histogram signal is more equally distributed for all channels, having an overall higher intensity for the frequency distribution. The differences in histograms profiles may be caused by different image formats and resolution of each device. These facts justify the application of calibration transfer to the data acquired, as without transfer technique, when the image from a device is validated into another, the result may be completely different.

In PLS, the number of latent variables (LV) was selected based on the smallest root mean square error of cross validation (RMSECV), using 3 LV. The prediction performance of a standard PLS calibration and figures of merit in the master (scanner) and slave (cell phone) devices are compared in Table 1. The plot of reference versus predicted values for each device is shown in Figure 3, showing the accuracy of the

models by comparing the means of the predicted concentration for validation set separately and after transfer technique. Standard-deviation found for validation set were quite low considering a triplicate, varying from 0 to 0.16 mg dL^{-1} for cell phone data and from 0.04 to 0.15mg dL^{-1} for scanned data.

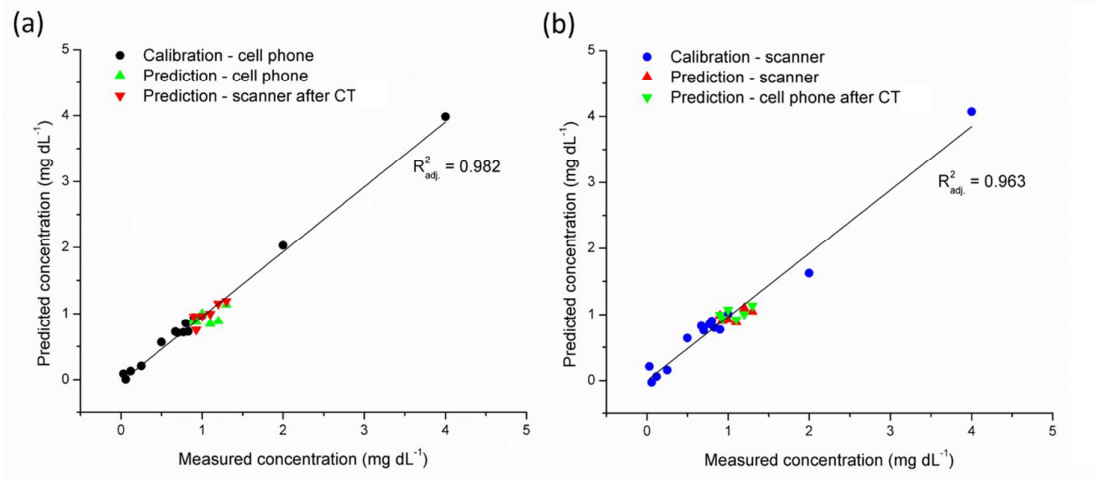

Figure 3: (a) Results of measured *versus* predicted concentration for PLS model for cell phone device: (●) calibration samples, (▲) prediction samples, and (▼) scanner prediction samples after calibration transfer; (b) Results of measured *versus* predicted concentration for PLS model for scanner device: (●) calibration samples, (▲) prediction samples, and (▼) cell phone prediction samples after calibration transfer.

Table 1: Results found for PLS models.

	Device	
Calibration parameters	Scanner	Cell phone
Number of latent variables	3	3
Variance explained (%)	97.94	99.73
Worked range (mg dL^{-1})	0.03 – 4.00	0.03 – 4.00
RMSECV (mg dL^{-1})	0.14	0.05
Bias at calibration (mg dL^{-1})	0.00	0.00
Prediction parameters		
RMSEP (mg dL^{-1})	0.15	0.18
Bias at prediction (mg dL^{-1})	0.10	0.13
Linearity		
Slope	0.979	0.997
Intercept	0.019	0.002
R	0.989	0.998
R^2	0.979	0.997

Trueness		
Relative error (%)	14.04	16.67
I_T[a]	0.886	0.842
Precision		
RSD(%)	2.60	4.76
I_P[a]	0.973	0.902
Accuracy		
Recovery(%)	91.67-100.00	86.67-91.67
β-TI	[-17.75; 1.12]	[-26.55%; 5.74%]
I_A	0.943	0.900
Others FOM		
LOD (mg dL^{-1})	0.08	0.11
LOQ (mg dL^{-1})	0.25	0.35
Analytical sensitivity (γ) (dL mg^{-1})	39.13	27.44
γ^{-1} (mg dL^{-1})	0.026	0.036
I_{DR}	0.972	0.960

[a]Trueness Index (I_T) and Precision Index (I_P) for an acceptable error of 15%.

PLS yielded the lowest RMSEP and the highest R and R^2 for all devices for the creatinine parameter. Accuracy values represented by RMSECV and RMSEP indicated the estimated PLS model values for each device showed excellent agreement with the enzymatic method. Some figures of merit results for PLS model of the cell phone and scanner are also provided in Table 1. Excellent results were observed for linear response, recovery and analytical sensitivity to the parameter evaluated, considering the analytical range of each model. The LOD and LOQ values observed for both devices were smaller than those obtained by the reference method for a protein sample containing creatinine (LOD and LOQ equals to 0.30 mg dL^{-1} and 0.99 mg dL^{-1}, respectively). The bias was only estimated for the validation set and shows a t-value (1.97) lower than the t-critical value (2.57, with 5 degrees of freedom and 95% confidence level), which indicates the absence of systematic errors in the model predictions. The values of the Trueness Index (I_T), Precision Index (I_P), Dosing Range

Index (I_{DR}) and Accuracy Index (I_A) were close to 1, meaning that the imaging method is almost non-biased, very precise, valid for the whole concentration range studied and shows good overall quality.[31] The β-TI estimated for each device can be seen in Table 1 and were based on three series of triplicates (p = 3 and n = 3). This indicates that it is expected that all the predicted values obtained for each model will present relative errors within the accepted limits, showing the reliability and feasibility of using image histograms from both devices to build a clinical method for analyzing creatinine in serum.

3.3 Transfer calibration

The results of the DS-PLS modelling procedure are shown in Fig. 4. In this graph, $RMSEP^{S}_{MT}$ is displayed as a function of the number of transfer samples (ranging from 1 to 14) using KS for the selection of transfer samples. The best result for creatinine ($RMSEP^{S}_{MT}$ = 0.10 mg dL^{-1}) was obtained by using DS-PLS with 12 transfer samples selected by KS.

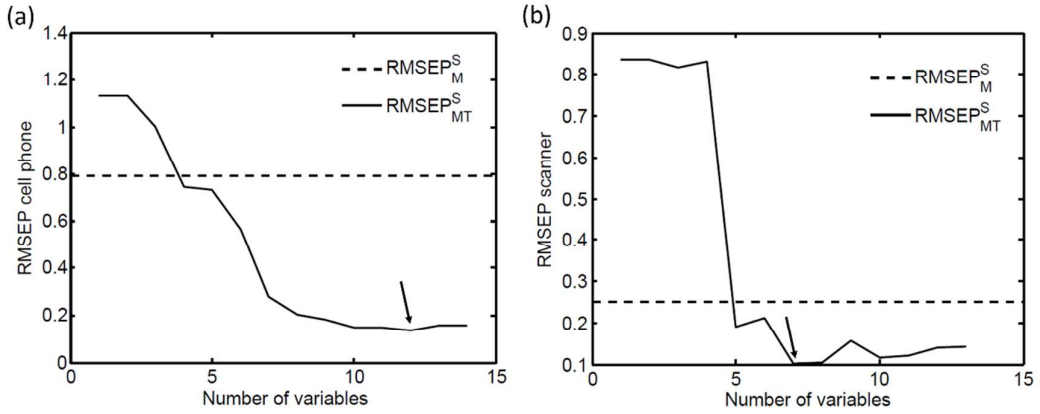

Figure 4. RMSEP value as a function of the number of transfer variables selected by KS algorithm of: (a) the cell phone device, employing the model calibrated for the scanner device. (b) the scanner device, employing the model calibrated for the cell phone device. The arrows indicate the minimum points used to choose the number of variables: (a) – 12 variables; (b) – 7 variables.

The prediction performance of a standard PLS calibration in the master (scanner) and slave (cell phone) devices after DS-PLS procedure are compared in Table 2. In addition, Table 2 shows the prediction performance using reverse standardization (RS) for cell phone data, where the prediction set of images acquired by scanner is applied to cell phone calibration model before and after RS-PLS.

Table 2: RMSEP, SEP, Bias and Relative error (%) for prediction set crossing samples for different devices and using calibration transfer by direct standardization (DS) for scanner data and reverse standardization (RS) for cell phone data.

	Scanner model (Master - M)		Cell phone model (Slave – S)[a]	
Prediction parameters	Prediction set cell phone (S)[b]	Prediction set cell phone (S-DS)[c]	Prediction set Scanner (M)[b]	Prediction set scanner (M-RS)[c]
RMSEP (mg dL^{-1})	0.79	0.14	0.25	0.10
Bias (mg dL^{-1})	0.78	0.06	0.24	0.07
Relative error (%)	73.31	12.66	23.13	9.40

[a]Cell phone model created by reverse standardization. [b]Before calibration transfer. [c]After calibration transfer.

As can be seen, Table 2 shows that the prediction accuracy (RMSEP, bias and relative error) of the PLS model is considerably improved when DS is applied to the histograms acquired from the cell phone device. The reduction from $RMSEP_M^S$ (0.79 mg dL^{-1}) to $RMSEP_{MT}^S$ (0.14 mg dL^{-1}) is very impressive, showing the importance of the transferable model and avoiding a full recalibration. In addition, there is a statistically significant reduction of the RMSEP value after RS for cell phone data being applied ($RMSEP_M^S$ = 0.25 mg dL^{-1} to $RMSEP_{MT}^S$ = 0.10 mg dL^{-1}). Likewise, the bias and relative error were improved after calibration transfer, especially when DS is applied to scanner data set.

4. Conclusion

A multivariate calibration method based on RGB, HSI and gray intensity histograms from digital images obtained from a cell phone and scanner was developed and validated for creatinine determination in serum samples. The results of this paper show that digital image analysis could be a substitute for the spectrophotometric measurements that have traditionally been used for creatinine assays of blood, using only a two-dimensional microplate array. This method was thoroughly validated in accordance with international guidelines, being considered as linear, accurate, unbiased, and suitable for use as an official methodology for creatinine determination in serum samples. In addition, this work supports the usefulness and effectiveness of calibration transfer method (DS-PLS) for the determination of biochemical assay (creatinine) using histograms obtained with low cost and from portable devices (cell phone and scanner).

Acknowledgements

Camilo de Lelis Medeiros de Morais thanks Propesq – PIBIC – UFRN and Conselho Nacional de Desenvolvimento Científico e Tecnológico (CNPq) for financial support. K.M.G. Lima acknowledges the CNPq/Capes project (Grant 070/2012 and 442087/2014-4) and FAPERN (PPP 005/2012) for financial support.

References

1 S. Ohtsuki, M. Tachikawa, H. Takanaga, H. Shimizu, M. Watanabe, K.-I. Hosoya and T. Terasaki, *J. Cereb. Blood Flow Metab.*, 2002, **22**, 1327–1335.

2 a Keppler, N. Gretz, R. Schmidt, H.-M. Kloetzer, H.-J. Groene, B. Lelongt, M. Meyer, M. Sadick and J. Pill, *Kidney Int.*, 2007, **71**, 74–78.

3 D. G. Robertson, M. D. Reily, R. E. Sigler, D. F. Wells, D. a Paterson and T. K. Braden, *Toxicol. Sci.*, 2000, **57**, 326–337.

4 R. A. Shaw, S. Low-Ying, M. Leroux and H. H. Mantsch, *Toward Reagent-free Clinical Analysis: Quantitation of Urine Urea, Creatinine, and Total Protein from the Mid-Infrared Spectra of Dried Urine Films*, 2000, vol. 46.

18

5 R. A. Shaw, S. Kotowich, H. H. Mantsch and M. Leroux, *Clin. Biochem.*, 1996, **29**, 11–19.

6 R. Stosch, A. Henrion, D. Schiel and B. Güttler, *Anal. Chem.*, 2005, **77**, 7386–7392.

7 K. Stojanova, R. Gulaboski, V. Mirečeski and S. Petrovska-Jovanović, *Anal. Lett.*, 1999, **32**, 2937–2950.

8 H. L. Lee and S. C. Chen, *Talanta*, 2004, **64**, 750–757.

9 E. P. Randviir, D. K. Kampouris and C. E. Banks, *Analyst*, 2013, **138**, 6565–72.

10 M. L. Knapp and P. D. Mayne, *Clin. Chim. Acta*, 1987, **168**, 239–246.

11 J. Castillo, H. Gutierrez, Y. Vitta, M. Martinez and A. Fernandez, *Adv. Environ. Chem. Biol. Sens. Technol. V*, 2007, **6755**, 67550W–1 – 67550W–9.

12 C. D. L. Medeiros de Morais and K. M. G. de Lima, *Talanta*, 2014, **126**, 145–50.

13 A. K. Yetisen, J. L. Martinez-Hurtado, A. Garcia-Melendrez, F. Da Cruz Vasconcellos and C. R. Lowe, *Sensors Actuators, B Chem.*, 2014, **196**, 156–160.

14 E. P. Moraes, N. S. A. Silva, C. D. L. M. De Morais, L. S. Neves and K. M. G. De Lima, *J. Chem. Educ.*, 2014, **91**, 1958–1960.

15 W. da Silva Lyra, F. A. Castriani Sanches, F. Antônio da Silva Cunha, P. H. Gonçalves Dias Diniz, S. G. Lemos, E. Cirino da Silva and M. C. Ugulino de Araujo, *Anal. Methods*, 2011, **3**, 1975.

16 W. Silva Lyra, V. B. dos Santos, A. G. G. Dionízio, V. L. Martins, L. F. Almeida, E. Nóbrega Gaião, P. H. G. D. Diniz, E. C. Silva and M. C. U. Araújo, *Talanta*, 2009, **77**, 1584–1589.

17 J. Manzano, D. Filippini and I. Lundström, 2004, 182–189.

18 B. M. a de Coninck, O. Amand, S. L. Delauré, S. Lucas, N. Hias, G. Weyens, J. Mathys, E. de Bruyne and B. P. a Cammue, *Plant Pathol.*, 2012, **61**, 76–84.

19 Y. Lu, W. Shi, J. Qin and B. Lin, *Electrophoresis*, 2009, **30**, 579–582.

20 P. H. G. D. Diniz, H. V. Dantas, K. D. T. Melo, M. F. Barbosa, D. P. Harding, E. C. L. Nascimento, M. F. Pistonesi, B. S. F. Band and M. C. U. Araújo, *Anal. Methods*, 2012, **4**, 2648.

21 F. Mendoza, N. A. Valous, P. Allen, T. A. Kenny, P. Ward and D. W. Sun, *Meat Sci.*, 2009, **81**, 313–320.

22 M. F. Abdelkader, J. B. Cooper and C. M. Larkin, *Chemom. Intell. Lab. Syst.*, 2012, **110**, 64–73.

19

23 R. N. Feudale, N. a. Woody, H. Tan, A. J. Myles, S. D. Brown and J. Ferré, *Chemom. Intell. Lab. Syst.*, 2002, **64**, 181–192.

24 J. Lin, S. C. Lo and C. W. Brown, *Anal. Chim. Acta*, 1997, **349**, 263–269.

25 F. Wulfert, W. T. Kok, O. E. de Noord and a. K. Smilde, *Anal. Chem.*, 2000, **72**, 1639–1644.

26. http://www.labtest.com.br/ (accessed July 2015)

27 G. L. Myers, W. G. Miller, J. Coresh, J. Fleming, N. Greenberg, T. Greene, T. Hostetter, A. S. Levey, M. Panteghini, M. Welch and J. H. Eckfeldt, *Clin. Chem.*, 2006, **52**, 5–18.

28. http://www.gimp.org / (accessed July 2015).

29 R. Kennard and L. Stone, *Technometric*, 1969, **11**, 137–148.

30 Y. Wang, D. J. Veltkamp and B. R. Kowalski, *Anal. Chem.*, 1991, **63**, 2750–2756.

31 E. Rozet, V. Wascotte, N. Lecouturier, V. Préat, W. Dewé, B. Boulanger and P. Hubert, *Anal. Chim. Acta*, 2007, **591**, 239–247.

32 J. Mantanus, E. Ziémons, E. Rozet, B. Streel, R. Klinkenberg, B. Evrard, J. Rantanen and P. Hubert, *Talanta*, 2010, **83**, 305–311.

33 B. G. Botelho, L. P. De Assis and M. M. Sena, *Food Chem.*, 2014, **159**, 175–180.

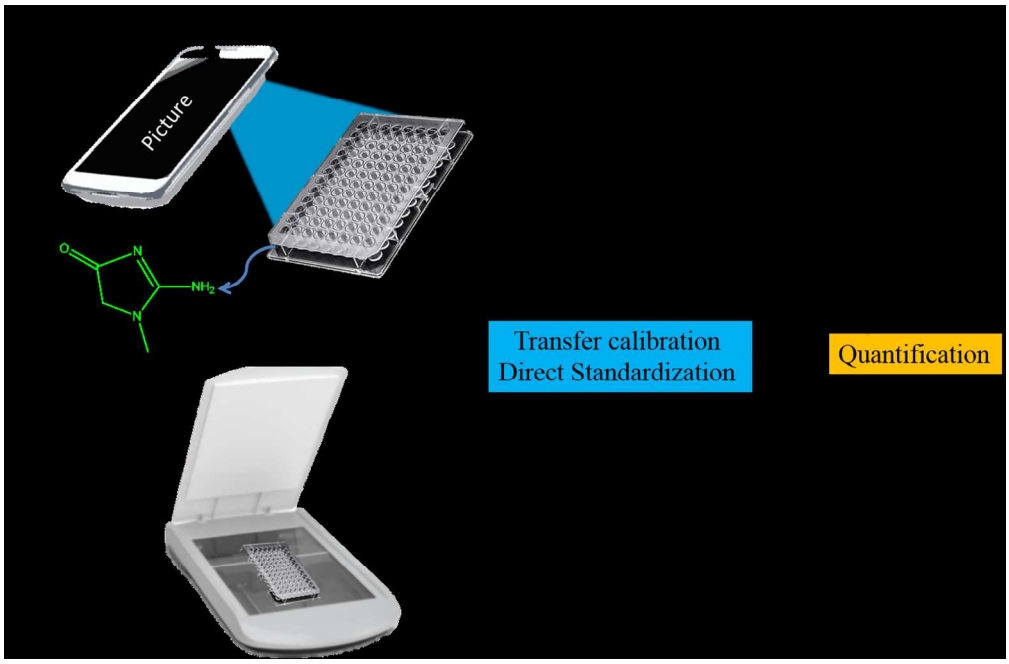

Graphical Abstract
121x79mm (300 x 300 DPI)